HHS Public Access

Author manuscript

Nucl Med Biol. Author manuscript; available in PMC 2019 March 01.

Published in final edited form as:

Nucl Med Biol. 2018 March ; 58: 67–73. doi:10.1016/j.nucmedbio.2017.12.004.

^{212}Pb-labeled B7-H3-targeting antibody for pancreatic cancer therapy in mouse models

Benjamin B. Kasten[1], **Abhishek Gangrade**[2], **Harrison Kim**[1], **Jinda Fan**[1], **Soldano Ferrone**[3], **Cristina R. Ferrone**[3], **Kurt R. Zinn**[4], and **Donald J. Buchsbaum**[2]

[1]Department of Radiology, University of Alabama at Birmingham, Birmingham, Alabama

[2]Department of Radiation Oncology, University of Alabama at Birmingham, Birmingham, Alabama

[3]Department of Surgery, Massachusetts General Hospital, Harvard Medical School, Boston, Massachusetts

[4]Institute for Quantitative Health Science and Engineering, Department of Radiology, Michigan State University, East Lansing, Michigan

Abstract

Introduction—We recently validated monoclonal antibody (mAb) 376.96 as an effective carrier for targeted α-particle radioimmunotherapy (RIT) with ^{212}Pb in ovarian cancer mouse models. In this study, we tested the binding of radiolabeled mAb 376.96 to human pancreatic ductal adenocarcinoma (PDAC) cells and localization in xenografts in immune-deficient mice and evaluated ^{212}Pb-labeled 376.96 (^{212}Pb-376.96) for PDAC therapy.

Methods—*In vitro* Scatchard assays assessed the specific binding of ^{212}Pb-376.96 to human PDAC3 adherent differentiated cells and non-adherent cancer initiating cells (CICs) dissociated from tumorspheres. *In vitro* clonogenic assays were used to measure the proliferation of adherent PDAC3 cells and CIC-enriched tumorspheres treated with ^{212}Pb-376.96 or the irrelevant isotype-matched ^{212}Pb-F3-C25. Mice bearing patient derived pancreatic cancer Panc039 xenografts were *i.v.* injected with 0.17–0.70 MBq ^{212}Pb-376.96 or isotype control ^{212}Pb-F3-C25, and used for biodistribution and tumor growth inhibition studies. Mice bearing orthotopic PDAC3 xenografts were *i.v.* co-injected with ^{99m}Tc-376.96 and ^{125}I-F3-C25 and used for biodistribution studies.

Results—^{212}Pb-376.96 specifically bound to PDAC3 adherent and dissociated tumorsphere CICs; K_d values averaged 9.0 and 21.7 nM, respectively, with 10^4-10^5 binding sites/cell. ^{212}Pb-376.96 inhibited the clonogenic survival of PDAC3 cells or CICs dissociated from tumorspheres 3–6 times more effectively than isotype-matched control ^{212}Pb-F3-C25. Panc039 *s.c.* tumors showed significantly higher uptake of ^{212}Pb-376.96 (14.0 ± 2.1% ID/g) compared to ^{212}Pb-F3-C25 (6.5 ± 0.9% ID/g, $p<0.001$) at 24 h after dosing. Orthotopic PDAC3 tumors showed

Corresponding author: Benjamin B. Kasten (postdoctoral trainee), University of Alabama at Birmingham, VH Box 601, 1720 2nd Ave South, Birmingham, AL 35294-0019, Phone: 205-996-5009, Fax: 205-975-6522, benjaminkasten@uabmc.edu.

Conflicts of interest: The authors declare no potential conflicts of interest.

significantly higher uptake of ^{99m}Tc-376.96 (6.4 ± 1.8% ID/g) compared to ^{125}I-F3-C25 (3.9 ± 0.9% ID/g, $p<0.05$) at 24 h after dosing. Panc039 tumor growth was significantly inhibited by ^{212}Pb-376.96 compared to ^{212}Pb-F3-C25 or non-treated control tumors ($p<0.05$).

Conclusion—Our results provide evidence for the efficacy of B7-H3 targeted RIT against preclinical models of pancreatic ductal adenocarcinoma (PDAC) and support future studies with ^{212}Pb-376.96 in combination with chemotherapy to potentiate efficacy against PDAC.

Keywords

Radioimmunotherapy; pancreatic ductal adenocarcinoma; ^{212}Pb; B7-H3

INTRODUCTION

Pancreatic ductal adenocarcinoma (PDAC) is estimated to cause over 43,000 deaths in the United States during 2017 and is associated with a 5-year survival rate of 8% [1]. The majority of patients (>80%) are diagnosed with locally advanced or metastatic disease that is not effectively controlled through surgical resection. Currently approved first-line chemotherapies (gemcitabine and *nab*-paclitaxel or FOLFIRINOX) are associated with median survivals of less than 1 year [2]. The high rate of invasive dissemination, the resistance of PDAC cells to chemotherapy, and the dense tumor stroma are notable obstacles contributing to the failure of conventional therapeutic strategies against PDAC. Thus, there has been a clinical demand for better treatment of this devastating disease. Cancer initiating cells (CICs), a subpopulation of tumor cells that are resistant to standard chemotherapy and are highly tumorigenic in immunedeficient mice [3, 4], have been implicated in the initiation and metastasis of PDAC. PDAC CICs and differentiated cells that survive chemotherapy contribute to the poor prognosis associated with PDAC [5]. Therefore, novel therapies that effectively target both differentiated PDAC cells and CICs may have great potential to improve therapeutic efficacy for PDAC [6, 7].

Targeted radioimmunotherapy (RIT) approaches with various radioimmunoconjugates (RICs) have been assessed against PDAC in preclinical and clinical studies [8, 9], although none have yet advanced to large-scale trials. Targeted RIT with α-particle emitting radionuclides is a promising approach to eliminate microscopic clusters of malignant cells due to the short path length (50–80 μm), high linear energy transfer (LET; 100 keV/μm), and high relative biological effectiveness of α-particles [10–12]. α-particles are known to induce cell death or proliferation arrest regardless of the cell's oxygen levels or sensitivity to chemotherapy or low LET (0.1–1 keV/μm) radiotherapy treatment (external beam or β-particle RIT) [11, 13]. These factors support the use of targeted α-particle RIT for locally advanced or metastatic PDACs that are resistant to first-line chemotherapies.

Targeted delivery of high LET radiation to both differentiated tumor cells and CICs represents a particularly attractive strategy to destroy malignant cells that survive alternative therapies while minimizing toxicities to normal tissues. The co-stimulatory protein B7-H3 (CD276) has been shown to be overexpressed in PDAC [14, 15], with higher expression correlating with aggressive and metastatic disease [16, 17]. PDAC cell lines and CICs express an extracellular B7-H3 epitope bound by monoclonal antibody (mAb) 376.96; this

epitope is not significantly expressed in normal tissues [4, 18], suggesting mAb 376.96 as a promising carrier for RIT of PDAC. Recent studies have demonstrated the efficacy of mAb 376.96 labeled with ^{212}Pb ($t_{1/2}$ = 10.64 h), which decays to the α-particle emitter ^{212}Bi ($t_{1/2}$ = 60.5 min), for targeted RIT in ovarian cancer mouse models [19, 20]. The goals of this investigation were to test the specific binding of radiolabeled mAb 376.96 to PDAC cells and localization in xenografts, and to evaluate ^{212}Pb-376.96 for pancreatic cancer therapy against PDAC mouse models.

MATERIALS AND METHODS

Reagents and instrumentation

All reagents were prepared from commercially available materials (Thermo Fisher, Sigma) unless specified otherwise. ^{212}Pb in transient equilibrium with its daughter radionuclides was eluted as previously described [21] from a ^{224}Ra/^{212}Pb generator obtained from Oak Ridge National Laboratory (Oak Ridge, TN). Murine mAb 376.96 [22] and isotype-matched control murine mAb F3-C25, an anti-idiotypic mAb to the murine anti-HLA Class II mAb CR11-462 [23], were produced and characterized as previously described. mAbs were purified from mouse ascites fluid by protein affinity chromatography. The purity and activity of mAb preparations were monitored by SDS-PAGE and by specific reactivity with the corresponding antigens in binding assays. An energy and efficiency calibrated high-purity germanium (HPGe) detector (model GMX10P4-70; Ortec, Oak Ridge, TN) operated at −4000 V housed in a lead shield (Ortec) was used to determine the radionuclidic purity and radioactivity of ^{212}Pb for all radiolabeling procedures. Spectra were processed using Gamma Vision-32 software (version 6.09; Ortec). Radioactivity measurements of samples from the *in vitro* and *in vivo* experiments were performed on calibrated Cobra II (Packard, Meriden, CT) or Wizard^2 (Perkin Elmer, Shelton, CT) gamma counters using an energy window centered on the main gamma peaks from ^{212}Pb (238.6 keV, 43.6%) or ^{212}Bi (727.3 keV, 6.7%) after cross-calibrating the instruments with the HPGe detector. Radioactivity analyses were corrected for radioactive decay.

Radiolabeling studies

mAbs 376.96 and F3-C25 were conjugated with the bifunctional chelator 2-(4-isothiocyanotobenzyl)-1,4,7,10-tetraaza-1,4,7,10-tetra-(2-carbamoylmethyl)-cyclododecane (TCMC; Macrocyclics, Plano, TX) following previously described procedures [24] to generate TCMC-mAb 376.96 and TCMC-mAb F3-C25. The average chelate/mAb ratios were determined by a spectrophotometric assay [25]. Radiolabeling and purification of the ^{212}Pb-TCMC-mAb RICs (^{212}Pb-376.96 or ^{212}Pb-F3-C25) were performed as previously described [21] using 0.12–0.3 MBq of ^{212}Pb in transient equilibrium with its daughter radionuclides per 1 μg of TCMC-mAb conjugate (18–44 GBq/μmol). Immediately after collecting the purified RICs, an aliquot was removed for additional characterization and 5 μL 0.1 mol/L EDTA and 50 μL 30% human serum albumin (Sigma-Aldrich, St. Louis, MO) were added to the RICs. The protein content of the removed aliquot was determined by Lowry analysis [26]. The radiochemical conversions and purities of the crude preparations and isolated RICs were determined as previously described [21]. mAb 376.96 containing 4.6 TCMC chelates per mAb was radiolabeled with ^{212}Pb to produce ^{212}Pb-376.96 in high yield

and radiochemical purity (84% and 98%, respectively, n=6) as indicated by ITLC analysis. The control mAb F3-C25 containing 5.6 TCMC chelates per mAb molecule was radiolabeled to give ^{212}Pb-F3-C25 with an average radiochemical purity of 93% (n=5). Procedures and results from *in vitro* stability analyses of ^{212}Pb-376.96 are provided in the Supplementary data (Supplementary Table S1). Specific activities of 74–204 kBq/μg (11–30 GBq/μmol) for the ^{212}Pb-RICs were used in the *in vitro* and *in vivo* studies described below. mAb 376.96 was conjugated with HYNIC-NHS and radiolabeled with ^{99m}Tc-tricine as previously described [27]; the isolated specific activity was 0.76 MBq/μg (81% radiochemical purity). mAb F3-C25 was radiolabeled with carrier-free Na^{125} I (MP Biomedicals, Solon, OH) in Pierce Pre-Coated Iodination Tubes (Thermo Scientific, Rockford, IL) according to manufacturer's specifications; the isolated specific activity was 46.6 kBq/μg (86% radiochemical purity).

Human PDAC3 cell line and CICs

The PDAC3 cell line established from ascites fluid of a human patient with metastatic PDAC, has been previously described [28]. Cells grown as monolayers ("Adherent" conditions) were cultured with high glucose DMEM medium supplemented with 10% fetal bovine serum (FBS; HyClone, Logan, UT) in tissue culture treated plates (Corning Costar, Corning, NY). Cells grown as non-adherent tumorspheres were cultured with serum-free high glucose DMEM supplemented with 20 μg/mL bovine insulin, 20 ng/mL epidermal growth factor, 10 ng/mL basic fibroblast growth factor, 5 μg/mL transferrin, 5 ng/mL sodium selenite, 16 μg/mL putrescene, and 7.3 ng/mL progesterone in ultra-low attachment plates (Corning Costar) as previously described to enrich for cells with characteristics of CIC proliferation [29, 30]; at 3 days after seeding cells in these conditions, compact spheroids with diameters of 35–65 μm and high cell viability (>95%) had formed. Cell culture and *in vitro* experiments were performed at 37 °C in a 5% CO_2 humidified atmosphere unless specified otherwise. Experiments were performed using cells under 15 passages from initial receipt and expansion; cells were discarded within 3 months of thawing the expanded frozen stocks.

In vitro binding assays

The binding of ^{212}Pb-376.96 to adherent PDAC3 cells and to PDAC3 cells dissociated from non-adherent tumorspheres grown under CIC conditions was tested as previously described for ovarian cancer cell lines to calculate the binding affinity (K_d), binding sites per cell, and internalized fraction [20, 27].

In vitro clonogenic survival assays

Adherent clonogenic assays—PDAC3 cells were seeded at 100,000 cells/well in 24-well plates (Corning Costar) two days before treatment with RICs, defined as day 0 of the study. On day 0, cells were rinsed with PBS and incubated with serial dilutions of ^{212}Pb-376.96 or ^{212}Pb-F3-C25 in 0.4 mL assay medium (DMEM pH 7.4 with 30 mmol/L HEPES, 2 mmol/L L-glutamine, 1 mmol sodium pyruvate, 1% bovine serum albumin) for 2 h at 37 °C with gentle swirling. Cells were rinsed twice with PBS and incubated in fresh Adherent medium. Two days later (day 2), cells were trypsinized, counted, serially diluted in

normal (Adherent) medium, and plated at 100 live cells/well in six replicate wells of a tissue culture treated 6-well plate (Corning Costar). The percent clonogenic survival relative to vehicle-treated controls was determined 10 days after plating (day 12) as previously described [20, 31].

CIC clonogenic assays—PDAC3 cells were seeded at 100,000 cells/well in 24-well ultra-low attachment plates in CIC conditions to form tumorspheres three days before treatment with RICs, defined as day 0 of the study. On day 0, intact tumorspheres (diameters of 35–65 μm) were collected, rinsed with PBS, and incubated with serial dilutions of ^{212}Pb-376.96 or ^{212}Pb-F3-C25 in 0.4 mL assay medium for 2 h at 37 °C with gentle swirling to keep tumorspheres in suspension. Tumorspheres were rinsed twice with PBS and incubated in new ultra-low attachment 24-well plates with fresh CIC medium. Two days later (day +2), tumorspheres were collected and dissociated into single cells with Accutase or trypsin, counted, and serially diluted in Adherent medium. Cells were plated and analyzed for clonogenic survival as in the Adherent clonogenic assays.

Animal subjects and husbandry

All *in vivo* studies were performed in 5–7 week old female athymic nude mice (Charles River, Wilmington, MA). Animal studies were approved by the University of Alabama at Birmingham Institutional Animal Care and Use Committee and performed in compliance with guidelines from the Public Health Service Policy and Animal Welfare Act of the United States. Sections (4×4×4 mm) of patient derived xenograft (PDX) Panc039 tumors propagated in the flank of nude mice as previously described [32] were implanted subcutaneously (*s.c.*) in mice. Radioactive biodistribution and therapy studies were initiated 4–5 weeks after implantation, when tumors had grown to 140–200 mm^3. PDAC3 cells (2.5×10^6) were implanted orthotopically into the pancreas of mice using previously described techniques [33]; biodistribution studies were performed 3 months after pancreas implantation, when tumors were 1.4–2.0 g. Mice were given Nutra-Gel Diet (Bio-Serv, Flemington, NJ) in addition to standard chow for two weeks after administering the RICs. Mice were weighed twice per week and euthanized if >10% weight loss occurred or when tumors grew to 1.5 cm in diameter. Tumor volume was calculated by the formula $(L\times W^2)/2$ as previously described [34].

In vivo biodistribution studies

Mice bearing *s.c.* PDX Panc039 tumors were injected *i.v.* with ~0.74 MBq (~4.0 μg) ^{212}Pb-376.96 or ^{212}Pb-F3-C25 (n = 4 mice/group) in 0.2 mL PBS. Mice bearing orthotopic PDAC3 tumors were intended for use in parallel biodistribution studies with ^{212}Pb-376.96 or ^{212}Pb-F3-C25, although variable rates of tumor development precluded using this PDAC xenograft model during the useable lifetime of the ^{224}Ra/^{212}Pb generator (see Discussion below). To test the localization of radiolabeled mAb 376.96 in the PDAC3 xenografts, mice bearing established tumors (n = 5 mice) were injected *i.v.* with a solution containing ^{99m}Tc-376.96 (6.02 MBq, 10.5 μg) and ^{125}I-F3-C25 (22.39 kBq, 10.6 μg) in 0.2 mL PBS. Mice were euthanized at 24 h post injection and selected tissues were removed and counted in a gamma counter. Percent uptake of the injected dose per gram (% ID/g) in all

experiments was calculated by comparing the tissue activity to solutions with known activity of the isotope of interest. ^{125}I was counted after ^{99m}Tc had fully decayed.

In vivo therapy studies

Groups of mice (n = 10/group) bearing *s.c.* Panc039 tumors were given a single *i.v.* dose of ^{212}Pb-376.96 or ^{212}Pb-F3-C25 (0.36–0.73 MBq) or received no treatment (control). Tumor growth was calculated as mean percent change in volume with standard error relative to the initial volume at the time of dosing.

Statistical analyses

Data were analyzed using Microsoft Excel or GraphPad Prism (Version 5.02). When comparing multiple groups, one-way or two-way ANOVA tests were performed, followed by Bonferroni tests to compare differences between individual groups. All p values correspond to two-tailed tests. $p<0.05$ was considered significant.

RESULTS

^{212}Pb-376.96 binds to differentiated human PDAC cells and human PDAC CICs

In vitro Scatchard binding assays showed ^{212}Pb-376.96 bound to adherent PDAC3 cells and to cells dissociated from non-adherent CIC tumorspheres with affinities of 9.0 ± 1.1 nM (n=6) and 21.7 ± 0.7 nM (n=3), respectively; specific binding was 73–76%. Representative binding results and Scatchard plots are shown in Figure 1. Significantly more binding sites/cell were present on the dissociated CICs compared to adherent cells (Table 1; $p<0.05$).

^{212}Pb-376.96 inhibits the clonogenic survival of differentiated human PDAC cells and human PDAC CICs *in vitro*

Adherent PDAC3 cells treated *in vitro* with ^{212}Pb-376.96 showed significantly lower clonogenic survival compared to cells treated with ^{212}Pb-F3-C25 (Table 2, $p<0.05$). Similarly, PDAC3 cells obtained from CIC tumorspheres were more sensitive to ^{212}Pb-376.96 than to ^{212}Pb-F3-C25 ($p=0.18$). Clonogenic survival following treatment with ^{212}Pb-F3-C25 was more variable than after treatment with ^{212}Pb-376.96. As shown in Table 2, the clonogenic survival of PDAC3 differentiated cells and CICs was inhibited 3–6 times more effectively by ^{212}Pb-376.96 than by ^{212}Pb-F3-C25.

^{212}Pb-376.96 targets human PDAC xenograft tumors *in vivo*

Mice with established *s.c.* PDX Panc039 tumors showed significantly higher uptake of the injected ^{212}Pb dose at 24 h after administration of ^{212}Pb-376.96 compared to the isotype control ^{212}Pb-F3-C25 (14.0 ± 2.1% and 6.5 ± 0.9% ID/g, respectively; $p<0.001$) (Figure 2A); the level of ^{212}Bi in the tumors was consistent with the activity of ^{212}Pb observed in both groups (Supplementary Tables S2 and S3). Mice in the ^{212}Pb-376.96 group showed uptake of ^{212}Pb in normal organs including spleen, liver, kidneys, and blood (18.2%, 9.8%, 10–14%, and 9.6% ID/g, respectively); mice in the ^{212}Pb-F3-C25 group showed comparable retention of ^{212}Pb in liver, kidneys, and blood (Figure 2A, Supplementary Tables S2 and S3). Mice in both groups showed higher retention of ^{212}Pb than ^{212}Bi in the liver, while more

^{212}Bi than ^{212}Pb was retained in the spleen, kidneys, blood, and femurs of mice from both groups (Supplementary Tables S2 and S3).

Orthotopic PDAC3 tumors showed significantly higher uptake of ^{99m}Tc-376.96 compared to ^{125}I-F3-C25 (6.4 ± 1.8% and 3.9 ± 0.9% ID/g, respectively, $p<0.05$) at 24 h after *i.v.* co-injection of the two radiolabeled antibodies (Figure 2B). The spleen showed high uptake of ^{99m}Tc-376.96, which correlated with the locally invasive growth of the orthotopic PDAC3 tumors into and around the spleen at the time of necropsy (data not shown). Biodistribution data for normal tissues and tumors are provided in Supplementary Table S4. These biodistribution results in different tumor models confirmed the effective and specific targeting of human PDAC with radiolabeled mAb 376.96.

^{212}Pb-376.96 significantly inhibits the growth of human PDX PDAC tumors *in vivo*

The uptake and targeting specificity of ^{212}Pb-376.96 in established Panc039 tumors suggested the relevant application of this RIT agent for treating solid PDAC tumors. Preliminary studies indicated that a single *i.v.* dose of 0.2–0.5 MBq ^{212}Pb-376.96 was well tolerated in mice and inhibited the growth of *s.c.* Panc039 tumors relative to non-treated controls (Supplementary Figure S1). For the experiments discussed here, tumor growth inhibition studies were performed in groups of *s.c.* Panc039 tumor-bearing mice given a single *i.v.* injection of 0.36, 0.54, or 0.73 MBq ^{212}Pb-376.96. Another group of tumor-bearing mice received a single *i.v.* injection of an intermediate dose of ^{212}Pb-F3-C25 (0.46 MBq) to determine the effects of non-targeted RIT against Panc039 tumors. All RIT treatments resulted in significant tumor growth inhibition relative to non-treated controls as early as day 9 ($p<0.05$) after injecting the RICs into mice, indicating the potency of ^{212}Pb RIT against this tumor model (Figure 3). The two higher doses of ^{212}Pb-376.96 (0.54 and 0.73 MBq) were significantly more effective at slowing tumor growth than the low dose (0.36 MBq) of ^{212}Pb-376.96 and 0.46 MBq dose of ^{212}Pb-F3-C25 as early as day 12 ($p<0.05$). This level of tumor growth inhibition continued throughout the period of the experiment, although no complete tumor regressions were observed. ^{212}Pb-376.96 at 0.36 MBq and the higher dose (0.46 MBq) of the control ^{212}Pb-F3-C25 were equally effective against Panc039 tumor growth (Figure 3). These results confirmed the growth inhibitory effects of B7-H3 targeted α-particle RIT against PDAC xenografts and also indicated the challenge of eradicating these established solid tumors under the conditions explored.

All treatments caused a transient drop in mice body weight; all groups of mice had recovered to their initial weight before treatment within 2 weeks after injecting the RICs (Supplementary Figure S2). At the end of the study period, the average percent increase in weights of mice treated with 0.54 or 0.73 MBq was slightly less than in mice from the non-treated control group (increase of 6.8 ± 4.0%, 10.0 ± 5.3%, and 16.3 ± 4.5%, respectively). These results indicate RIT with ^{212}Pb-376.96 was generally well tolerated at the dose levels and time frames explored, although toxicology effects on blood parameters or normal organs have yet to be characterized.

DISCUSSION

The studies presented here are unique in that the RIC targets a tumor-specific B7-H3 antigen expressed on CICs and differentiated tumor cells from multiple models of PDAC [4, 18]. ^{212}Pb-376.96 bound to PDAC3 cells with similar affinities as previously shown in ovarian cancer cell lines, although fewer binding sites per cell were present on the PDAC3 cells compared to ovarian cancer cells [20]. Of interest, the dissociated cells from CIC tumorspheres exposed to ^{212}Pb-376.96 showed lower clonogenic survival than adherent PDAC3 cells exposed to ^{212}Pb-376.96. This could be due to the higher number of binding sites on the CICs relative to adherent cells and to the bystander effect of α-particles emitted from an antigen-bound RIC into the highly compact CIC tumorsphere, as a single α-particle would be expected to traverse the entire diameter of the PDAC3 tumorsphere (<70 μm). The 3–6 fold greater sensitivity of PDAC3 cells to ^{212}Pb-376.96 relative to the control ^{212}Pb-F3-C25 is comparable to that observed with ^{212}Pb-trastuzumab relative to a control RIC in alternative PDAC cell lines [10]. PDAC3 adherent cells and CICs were slightly less sensitive than ovarian cancer cells to ^{212}Pb-376.96 [20]. These differences are likely due to disparities in antigen expression, cell size, and activation of repair mechanisms between the cell lines.

The biodistribution studies in two PDAC models showed significantly higher tumor accumulation of ^{212}Pb-376.96 or ^{99m}Tc-376.96 compared to the isotype control RICs. These results verified the utility of mAb 376.96 for targeting the B7-H3 epitope in these PDAC models. Both the PDAC3 and Panc039 tumor models were intended for use in parallel biodistribution studies with ^{212}Pb-376.96, although the variable rate of PDAC3 tumor growth prohibited experiments with these tumors during the usable lifetime of the ^{224}Ra/^{212}Pb generator. ^{203}Pb ($t_{1/2}$ = 51.9 h; 279.2 keV, 80.9%) has favorable properties for SPECT imaging and could be used as a matched-pair diagnostic radionuclide for ^{212}Pb RIT applications; however, this radionuclide was not available at the time this study was carried out. Biodistribution studies in mice with PDAC3 tumors used ^{99m}Tc and ^{125}I due to their low cost and well-characterized radiolabeling properties. It is recognized that using different radionuclides could impact the relative biodistribution of the RICs. The lower uptake of ^{99m}Tc-376.96 in the PDAC3 tumors compared to ^{212}Pb-376.96 in the Panc039 tumors was likely due to the large size of the PDAC3 tumors (>1.5 g) at the time of the study.

The previous TCMC-mAb 376.96 conjugate used in the studies with intraperitoneal (*i.p.*) models of ovarian cancer [20] had a high chelate/mAb ratio (12.7) that was similar to the chelate/mAb ratio (14.0) of the ^{212}Pb-TCMC-trastuzumab conjugate used for *i.p.* injection in the non-human primate and human clinical trials [35–38]. As the ^{212}Pb-RICs in the current studies were intended for *i.v.* rather than *i.p.* injection, lower chelate/mAb ratios (4.6–5.6) were used to reduce potential retention of the RICs in the reticuloendothelial system (RES) after systemic injection [39, 40]. The uptake of ^{212}Pb and ^{212}Bi in the spleens of mice in the current biodistribution studies with ^{212}Pb-376.96 was comparable to that observed in our previous study for this IgG_{2a} isotype RIC [20]. The observed differences in normal tissue retention between ^{212}Pb and its daughter ^{212}Bi are consistent with previous studies that systemically administered ^{212}Pb-labeled compounds [41, 42]; ~30% of ^{212}Bi has been shown to be released from the original ^{212}Pb-chelate complex due to internal conversion during decay of ^{212}Pb [43], which would allow distribution of free ^{212}Bi and its

daughter radionuclides during circulation of the ^{212}Pb-RICs. Several strategies could be employed to minimize the amount of systemically released ^{212}Bi emitted from ^{212}Pb-conjugates, such as employing small targeting carriers that have rapid pharmacokinetics when *i.v.* injections are required [41, 42], targeting intracavitary (e.g., *i.p.*) lesions with local administrations when using mAbs as targeting vectors [10, 35, 36, 44], or other approaches to control recoiling daughter radionuclides that emit α-particles [45].

Prior studies have not explored α-particle RIC biodistribution and therapeutic efficacy using a macroscopic PDX PDAC tumor model *in vivo*. The high Panc039 tumor uptake and relatively low normal tissue retention of ^{212}Pb-376.96 relative to the control RIC in the present studies supported the potential efficacy of targeted RIT against this PDAC model with tolerable levels of ^{212}Pb-376.96. The partial growth inhibition of the Panc039 tumors by the control RIC suggests efficacy may be due to disruption of tumor vasculature by α-particles emitted from circulating ^{212}Pb-RICs, or to killing of tumor and stromal cells from ^{212}Pb-RICs that extravasated through leaky vessels within the tumors. Several studies have shown inhibition of tumor growth from control mAbs labeled with ^{212}Pb [46, 47] or other radionuclides [48]. Dosimetry analyses would be helpful in estimating the relative efficacy of the targeted or control ^{212}Pb-RICs in future studies. In addition to target antigen expression on PDAC cells, it is possible that the B7-H3 antigen targeted by mAb 376.96 is also expressed in the vasculature of the Panc039 xenografts; B7-H3 expression has been characterized in the tumor vasculature of several malignancies [49–51], although antigen expression in PDAC vasculature has not yet been confirmed. Future work that explores the effects of ^{212}Pb-376.96 on PDAC tumor vasculature would help elucidate the mechanism of this RIT strategy beyond killing small clusters of tumor cells.

Several studies have investigated the efficacy of α-particle RIT against preclinical models of PDAC [8, 10, 52–56]. Studies that initiated treatment soon (<3 days) after *s.c.* PDAC xenograft implantation before macroscopic tumor burden had developed showed that tolerable doses of targeted ^{213}Bi-RICs were able to prevent tumor formation, indicating therapeutic efficacy in these scenarios of sub-clinical PDAC foci [53–55]. Studies that initiated treatment with targeted ^{212}Pb- or ^{213}Bi-RICs at later time points (>6 days) after *i.p.* xenograft implantation when disseminated PDAC burden was established showed moderate efficacy and specificity relative to non-targeted RICs; PDAC tumor burden progressed in all animals under the conditions explored [10, 52]. Studies using targeted ^{213}Bi-RIT or brachytherapy with ^{224}Raimplanted rods in macroscopic *s.c.* PDAC tumors showed delayed tumor growth due to therapy, although tumor progression was not eradicated in these studies [56, 57]. The RIT results presented above with ^{212}Pb-376.96 against macroscopic PDAC tumors are consistent with these previous studies, indicating the significant challenge to eradicate established PDAC with a single administration of α-particle RICs. While the limited tissue penetration of α-particles is not ideal for treating large solid tumors, preclinical studies have proven the concept that fractionated RIT with short-lived α-particle radionuclides can eradicate macroscopic human xenograft tumors in mice [58]. These results support future investigations of fractionated dosing schedules and combinatorial chemotherapy regimens with ^{212}Pb-376.96 against PDAC.

Performing the *in vitro* assays with a single PDAC cell line is a limitation noted for the studies above; previous work has shown that several PDAC cell lines express the B7-H3 antigen bound by mAb 376.96 [4, 18], suggesting additional cell lines would be suitable for inclusion in future studies with ^{212}Pb-376.96. Limitations for the *in vivo* studies include the modest specificity of tumor growth inhibition with ^{212}Pb-376.96 relative to ^{212}Pb-F3-C25. The relatively large starting size of the tumors, limited tissue extravasation of mAbs, and the short tissue penetration of α-particles, including those emitted from RICs bound to the tumor antigen, are factors that could have detracted from therapeutic efficacy of the targeted RIC relative to the control RIC. It should be noted that a lower dose of ^{212}Pb-376.96 produced an equivalent inhibition in Panc039 tumor growth as a higher dose of ^{212}Pb-F3-C25. Such a benefit of targeted ^{212}Pb RIT relative to non-specific RIT was greater than that observed in a previous study that used a large, established *s.c.* ovarian tumor model [34]. Dosimetry and toxicology analyses were beyond the scope of the present studies, which were intended as the initial step to investigate the potential for mAb 376.96 as a carrier for ^{212}Pb RIT of PDAC. Future studies will define dosimetry and toxicology parameters and will determine if fractionated doses of ^{212}Pb-376.96 alone or in combination with chemotherapy and inhibitors of CIC proliferation can cause tumor regression in preclinical models of human PDAC. These additional preclinical studies would be essential prior to clinical assessment of mAb 376.96 as a targeting agent for RIT. As murine mAbs typically induce immunogenic responses in humans, humanization of mAb 376.96 would be needed prior to assessment of fractionated dosing regimens in humans.

CONCLUSION

The results from the above studies support the concept for B7-H3 targeted RIT with ^{212}Pb-376.96 against preclinical models of PDAC. ^{212}Pb-376.96 specifically bound to and inhibited the growth of PDAC cells and CICs *in vitro* as well as established patient derived PDAC tumor xenografts *in vivo*. The aberrant overexpression of B7-H3 in multiple malignancies [59, 60] suggests using mAb 376.96 as a carrier for targeted RIT would be worthy of exploration beyond the ovarian and PDAC models examined to date.

Supplementary Material

Refer to Web version on PubMed Central for supplementary material.

Acknowledgments

Jeffrey Sellers, Sharon Samuel, Sheila Bright, Cherlene Hardy, Debbie Della Manna, Quentin Whittsit, Sivaram Sridharan, Jillian Richter, Carey Hickerson, Marie Warren, Patsy Oliver, and Karim Budhwani are gratefully acknowledged for their contributions. The ^{212}Pb used in this research was obtained from a ^{224}Ra/^{212}Pb generator supplied by the United States Department of Energy Office of Science by the Isotope Program in the Office of Nuclear Physics.

Financial support: Funding was provided by NIH grant R21CA173120 and the Comprehensive Cancer Center at the University of Alabama at Birmingham.

References

1. American Cancer Society. Cancer Facts and Figures 2017. 2017.

2. Ghosn M, Ibrahim T, Assi T, El Rassy E, Kourie HR, Kattan J. Dilemma of first line regimens in metastatic pancreatic adenocarcinoma. World J Gastroenterol. 2016; 22:10124–30. [PubMed: 28028360]
3. Reya T, Morrison SJ, Clarke MF, Weissman IL. Stem cells, cancer, and cancer stem cells. Nature. 2001; 414:105–11. [PubMed: 11689955]
4. Wang, Y., Sabbatino, F., Yu, L., Favoino, E., Wang, X., Ligorio, M., et al. Tumor antigen-specific monoclonal antibody-based immunotherapy, cancer initiating cells and disease recurrence. In: Bonavida, B., editor. Resistance to Immunotherapeutic Antibodies in Cancer. Springer; New York: 2013. p. 25-47.
5. Ercan G, Karlitepe A, Ozpolat B. Pancreatic cancer stem cells and therapeutic approaches. Anticancer Res. 2017; 37:2761–75. [PubMed: 28551612]
6. Huang EH, Heidt DG, Li CW, Simeone DM. Cancer stem cells: a new paradigm for understanding tumor progression and therapeutic resistance. Surgery. 2007; 141:415–9. [PubMed: 17383517]
7. Krantz SB, Shields MA, Dangi-Garimella S, Munshi HG, Bentrem DJ. Contribution of epithelial-to-mesenchymal transition and cancer stem cells to pancreatic cancer progression. J Surg Res. 2012; 173:105–12. [PubMed: 22099597]
8. Sahlin M, Bauden MP, Andersson R, Ansari D. Radioimmunotherapy—a potential novel tool for pancreatic cancer therapy? Tumor Biol. 2015; 36:4053–62.
9. Shah M, Da Silva R, Gravekamp C, Libutti SK, Abraham T, Dadachova E. Targeted radionuclide therapies for pancreatic cancer. Cancer Gene Ther. 2015; 22:375–9. [PubMed: 26227823]
10. Milenic DE, Garmestani K, Brady ED, Albert PS, Ma D, Abdulla A, et al. α-particle radioimmunotherapy of disseminated peritoneal disease using a ^{212}Pb-labeled radioimmunoconjugate targeting HER2. Cancer Biother Radiopharm. 2005; 20:557–68. [PubMed: 16248771]
11. Elgqvist J, Frost S, Pouget J-P, Albertsson P. The potential and hurdles of targeted alpha therapy - clinical trials and beyond. Front Oncol. 2014; 3:324.doi: 10.3389/fonc.2013.00324 [PubMed: 24459634]
12. Palm S, Bäck T, Haraldsson B, Jacobsson L, Lindegren S, Albertsson P. Biokinetic modeling and dosimetry for optimizing intraperitoneal radioimmunotherapy of ovarian cancer microtumors. J Nucl Med. 2016; 57:594–600. [PubMed: 26769860]
13. Yong K, Brechbiel M. Application of ^{212}Pb for targeted alpha-particle therapy (TAT): Pre-clinical and mechanistic understanding through to clinical translation. AIMS Med Sci. 2015; 2:228–45. [PubMed: 26858987]
14. Loos M, Hedderich DM, Ottenhausen M, Giese NA, Laschinger M, Esposito I, et al. Expression of the costimulatory molecule B7-H3 is associated with prolonged survival in human pancreatic cancer. BMC Cancer. 2009; 9:463. [PubMed: 20035626]
15. Chen Y, Sun J, Zhao H, Zhu D, Zhi Q, Song S, et al. The coexpression and clinical significance of costimulatory molecules B7-H1, B7-H3, and B7-H4 in human pancreatic cancer. Onco Targets Ther. 2014; 7:1465–72. [PubMed: 25170273]
16. Yamato I, Sho M, Nomi T, Akahori T, Shimada K, Hotta K, et al. Clinical importance of B7-H3 expression in human pancreatic cancer. Br J Cancer. 2009; 101:1709–16. [PubMed: 19844235]
17. Zhao XIN, Li D-C, Zhu X-G, Gan W-J, Li ZHI, Xiong F, et al. B7-H3 overexpression in pancreatic cancer promotes tumor progression. Int J Mol Med. 2013; 31:283–91. [PubMed: 23242015]
18. Sabbatino F, Wang Y, Wang X, Schwab JH, Ferrone S, Ferrone CR. Novel tumor antigen-specific monoclonal antibody-based immunotherapy to eradicate both differentiated cancer cells and cancer-initiating cells in solid tumors. Semin Oncol. 2014; 41:685–99. [PubMed: 25440613]
19. Kasten B, Katre A, Kim H, Arend R, Fan J, Ferrone S, et al. Targeted radioimmunotherapy with B7-H3-specific ^{212}Pb-mAb 376.96 in models of human ovarian cancer. J Nucl Med. 2016; 57:55.
20. Kasten BB, Arend RC, Katre AA, Kim H, Fan J, Ferrone S, et al. B7-H3-targeted ^{212}Pb radioimmunotherapy of ovarian cancer in preclinical models. Nucl Med Biol. 2017; 47:23–30. [PubMed: 28104527]
21. Baidoo KE, Milenic DE, Brechbiel MW. Methodology for labeling proteins and peptides with lead-212 (^{212}Pb). Nucl Med Biol. 2013; 40:592–9. [PubMed: 23602604]

22. Imai K, Wilson BS, Bigotti A, Natali PG, Ferrone S. A 94,000-dalton glycoprotein expressed by human melanoma and carcinoma cells. J Natl Cancer Inst. 1982; 68:761–9. [PubMed: 6951087]
23. Perosa F, Ferrone S. Syngeneic anti-idiotypic antisera to murine anti-HLA Class II monoclonal antibodies. J Immunol. 1987; 139:1232–9. [PubMed: 3611788]
24. Chappell LL, Dadachova E, Milenic DE, Garmestani K, Wu C, Brechbiel MW. Synthesis, characterization, and evaluation of a novel bifunctional chelating agent for the lead isotopes ^{203}Pb and ^{212}Pb. Nucl Med Biol. 2000; 27:93–100. [PubMed: 10755652]
25. Dadachova E, Chappell LL, Brechbiel MW. Spectrophotometric method for determination of bifunctional macrocyclic ligands in macrocyclic ligand-protein conjugates. Nucl Med Biol. 1999; 26:977–82. [PubMed: 10708314]
26. Lowry OH, Rosebrough NJ, Farr AL, Randall RJ. Protein measurement with the folin phenol reagent. J Biol Chem. 1951; 193:265–75. [PubMed: 14907713]
27. Kim H, Zhai G, Liu Z, Samuel S, Shah N, Helman EE, et al. EMMPRIN as a novel target for pancreatic cancer therapy. Anticancer Drugs. 2011; 22:864–74. [PubMed: 21730821]
28. Perera RM, Stoykova S, Nicolay BN, Ross KN, Fitamant J, Boukhali M, et al. Transcriptional control of autophagy-lysosome function drives pancreatic cancer metabolism. Nature. 2015; 524:361–5. [PubMed: 26168401]
29. Dalerba P, Cho RW, Clarke MF. Cancer stem cells: Models and concepts. Annu Rev Med. 2007; 58:267–84. [PubMed: 17002552]
30. Schultz MJ, Holdbrooks AT, Chakraborty A, Grizzle WE, Landen CN, Buchsbaum DJ, et al. The tumor-associated glycosyltransferase ST6Gal-I regulates stem cell transcription factors and confers a cancer stem cell phenotype. Cancer Res. 2016; 76:3978–88. [PubMed: 27216178]
31. Bose RN, Maurmann L, Mishur RJ, Yasui L, Gupta S, Grayburn WS, et al. Non-DNA-binding platinum anticancer agents: Cytotoxic activities of platinum–phosphato complexes towards human ovarian cancer cells. Proc Natl Acad Sci U S A. 2008; 105:18314–9. [PubMed: 19020081]
32. Kim H, Samuel S, Lopez-Casas P, Grizzle W, Hidalgo M, Kovar J, et al. SPARC-independent delivery of nab-paclitaxel without depleting tumor stroma in patient-derived pancreatic cancer xenografts. Mol Cancer Ther. 2016; 15:680–8. [PubMed: 26832793]
33. Kim H, Folks KD, Guo L, Sellers JC, Fineberg NS, Stockard CR, et al. Early therapy evaluation of combined cetuximab and irinotecan in orthotopic pancreatic tumor xenografts by dynamic contrast-enhanced magnetic resonance imaging. Mol Imaging. 2011; 10:153–67. [PubMed: 21496446]
34. Horak E, Hartmann F, Garmestani K, Wu C, Brechbiel M, Gansow OA, et al. Radioimmunotherapy targeting of HER2/neu oncoprotein on ovarian tumor using lead-212-DOTA-AE1. J Nucl Med. 1997; 38:1944–50. [PubMed: 9430475]
35. Meredith R, Torgue J, Shen S, Fisher DR, Banaga E, Bunch P, et al. Dose escalation and dosimetry of first-in-human α radioimmunotherapy with ^{212}Pb-TCMC-trastuzumab. J Nucl Med. 2014; 55:1636–42. [PubMed: 25157044]
36. Meredith RF, Torgue J, Azure MT, Shen S, Saddekni S, Banaga E, et al. Pharmacokinetics and imaging of ^{212}Pb-TCMC-trastuzumab after intraperitoneal administration in ovarian cancer patients. Cancer Biother Radiopharm. 2014; 29:12–7. [PubMed: 24229395]
37. Kasten BB, Azure MT, Schoeb TR, Fisher DR, Zinn KR. Imaging, biodistribution, and toxicology evaluation of ^{212}Pb-TCMC-trastuzumab in nonhuman primates. Nucl Med Biol. 2016; 43:391–6. [PubMed: 27179247]
38. Meredith RF, Torgue JJ, Rozgaja TA, Banaga EP, Bunch PW, Alvarez RD, et al. Safety and outcome measures of first-in-human intraperitoneal α radioimmunotherapy with ^{212}Pb-TCMC-trastuzumab. Am J Clin Oncol. 2016; doi: 10.1097/COC.0000000000000353
39. Kukis DL, DeNardo GL, DeNardo SJ, Mirick GR, Miers LA, Greiner DP, et al. Effect of the extent of chelate substitution on the immunoreactivity and biodistribution of 2IT-BAT-Lym-1 immunoconjugates. Cancer Res. 1995; 55:878–84. [PubMed: 7850803]
40. Al-Ejeh F, Darby JM, Thierry B, Brown MP. A simplified suite of methods to evaluate chelator conjugation of antibodies: Effects on hydrodynamic radius and biodistribution. Nucl Med Biol. 2009; 36:395–402. [PubMed: 19423007]

41. Miao Y, Hylarides M, Fisher DR, Shelton T, Moore H, Wester DW, et al. Melanoma therapy via peptide-targeted α-radiation. Clin Cancer Res. 2005; 11:5616–21. [PubMed: 16061880]
42. Su FM, Beaumier P, Axworthy D, Atcher R, Fritzberg A. Pretargeted radioimmunotherapy in tumored mice using an in vivo ^{212}Pb/^{212}Bi generator. Nucl Med Biol. 2005; 32:741–7. [PubMed: 16243650]
43. Mirzadeh S, Kumar K, Gansow Otto A. The Chemical Fate of ^{212}Bi-DOTA Formed by β^- Decay of ^{212}Pb(DOTA)$^{2-}$. Radiochim Acta. 1993:1–10.
44. Milenic D, Molinolo A, Solivella M, Banaga E, Torgue J, Besnainou S, et al. Toxicological studies of ^{212}Pb intravenously or intraperitoneally injected into mice for a phase 1 trial. Pharmaceuticals. 2015; 8:416–34. [PubMed: 26213947]
45. de Kruijff RM, Wolterbeek HT, Denkova AG. A critical review of alpha radionuclide therapy—how to deal with recoiling daughters? Pharmaceuticals. 2015; 8:321–36. [PubMed: 26066613]
46. Milenic DE, Baidoo KE, Shih JH, Wong KJ, Brechbiel MW. Evaluation of platinum chemotherapy in combination with HER2-targeted α-particle radiation. Cancer Biother Radiopharm. 2013; 28:441–9. [PubMed: 23758610]
47. Yong KJ, Milenic DE, Baidoo KE, Brechbiel MW. Sensitization of tumor to ^{212}Pb radioimmunotherapy by gemcitabine involves initial abrogation of G2 arrest and blocked DNA damage repair by interference with Rad51. Int J Radiat Oncol, Biol, Phys. 2013; 85:1119–26. [PubMed: 23200172]
48. Sharkey RM, Karacay H, Govindan SV, Goldenberg DM. Combination radioimmunotherapy and chemoimmunotherapy involving different or the same targets improves therapy of human pancreatic carcinoma xenograft models. Mol Cancer Ther. 2011; 10:1072–81. [PubMed: 21467164]
49. Seaman S, Stevens J, Yang MY, Logsdon D, Graff-Cherry C, St Croix B. Genes that distinguish physiological and pathological angiogenesis. Cancer Cell. 2007; 11:539–54. [PubMed: 17560335]
50. Crispen PL, Sheinin Y, Roth TJ, Lohse CM, Kuntz SM, Frigola X, et al. Tumor cell and tumor vasculature expression of B7-H3 predict survival in clear cell renal cell carcinoma. Clin Cancer Res. 2008; 14:5150–7. [PubMed: 18694993]
51. Zang X, Sullivan PS, Soslow RA, Waitz R, Reuter VE, Wilton A, et al. Tumor associated endothelial expression of B7-H3 predicts survival in ovarian carcinomas. Mod Pathol. 2010; 23:1104–12. [PubMed: 20495537]
52. Milenic DE, Garmestani K, Brady ED, Albert PS, Ma D, Abdulla A, et al. Targeting of HER2 antigen for the treatment of disseminated peritoneal disease. Clin Cancer Res. 2004; 10:7834–41. [PubMed: 15585615]
53. Qu CF, Song EY, Li Y, Rizvi SMA, Raja C, Smith R, et al. Pre-clinical study of ^{213}Bi labeled PAI2 for the control of micrometastatic pancreatic cancer. Clin Exp Metastasis. 2005; 22:575–86. [PubMed: 16475028]
54. Qu CF, Song YJ, Rizvi SMA, Li Y, Smith R, Perkins A, et al. In vivo and in vitro inhibition of pancreatic cancer growth by targeted alpha therapy using ^{213}Bi-CHX.A"-C595. Cancer Biol Ther. 2005; 4:848–53. [PubMed: 16082185]
55. Allen BJ, Abbas Rizvi SM, Qu CF, Smith RC. Targeted alpha therapy approach to the management of pancreatic cancer. Cancers. 2011; 3:1821–43. [PubMed: 24212784]
56. Bryan RA, Jiang Z, Jandl T, Strauss J, Koba W, Onyedika C, et al. Treatment of experimental pancreatic cancer with 213-bismuth-labeled chimeric antibody to single-strand DNA. Expert Rev Anticancer Ther. 2014; 14:1243–9. [PubMed: 25156106]
57. Horev-Drori G, Cooks T, Bittan H, Lazarov E, Schmidt M, Arazi L, et al. Local control of experimental malignant pancreatic tumors by treatment with a combination of chemotherapy and intratumoral ^{224}Radium-loaded wires releasing alpha-emitting atoms. Transl Res. 2012; 159:32–41. [PubMed: 22153808]
58. Bäck T, Chouin N, Lindegren S, Kahu H, Jensen H, Albertsson P, et al. Cure of human ovarian carcinoma solid xenografts by fractionated α-radioimmunotherapy with ^{211}At-MX35-F(ab′)$_2$: Influence of absorbed tumor dose and effect on long-term survival. J Nucl Med. 2017; 58:598–604. [PubMed: 27688477]

59. Picarda E, Ohaegbulam KC, Zang X. Molecular pathways: Targeting B7-H3 (CD276) for human cancer immunotherapy. Clin Cancer Res. 2016; 22:3425–31. [PubMed: 27208063]

60. Castellanos JR, Purvis IJ, Labak CM, Guda MR, Tsung AJ, Velpula KK, et al. B7-H3 role in the immune landscape of cancer. Am J Clin Exp Immunol. 2017; 6:66–75. [PubMed: 28695059]

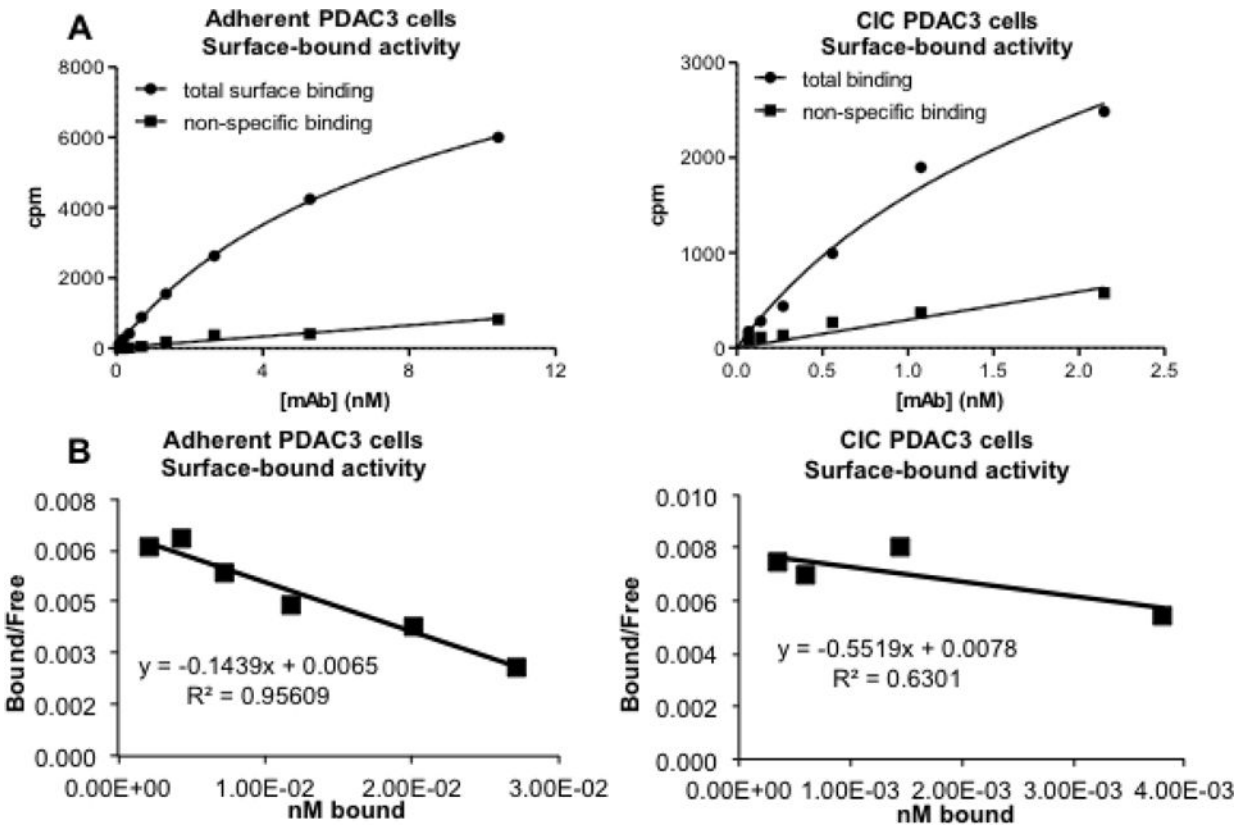

Figure 1.

Representative graphs showing *in vitro* binding of ^{212}Pb-376.96 to PDAC3 cells and CICs (A) and Scatchard plots of the data (B).

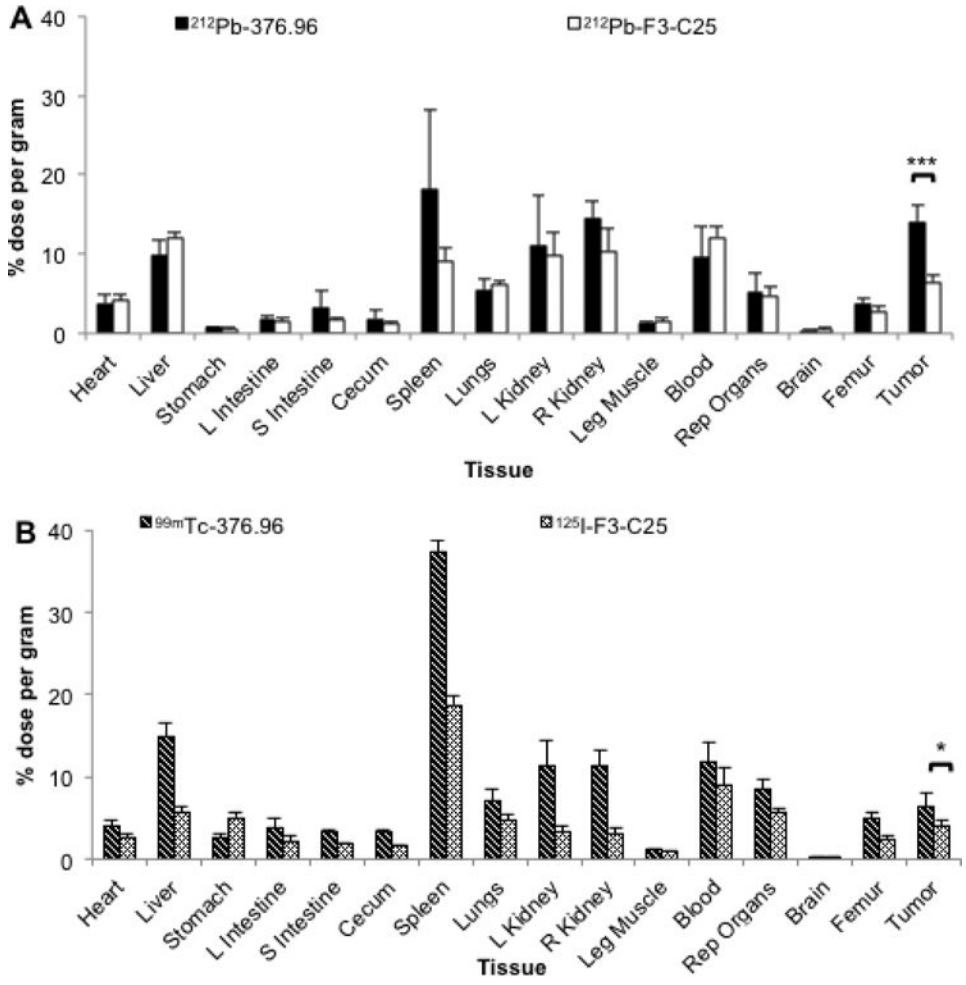

Figure 2.

Biodistribution analyses in mice with PDAC xenograft tumors. (A) Biodistribution at 24 h after *i.v.* injection of ^{212}Pb-376.96 or ^{212}Pb-F3-C25 (0.74 MBq) in groups of athymic nude mice (n = 4/group) bearing *s.c.* PDX Panc039 tumors. (B) Biodistribution at 24 h after *i.v.* co-injection of ^{99m}Tc-376.96 (6.02 MBq) and ^{125}I-F3-C25 (22.39 kBq) in athymic nude mice (n = 5 mice) bearing orthotopic PDAC3 tumors; ^{125}I was counted after ^{99m}Tc had fully decayed. After euthanization of mice, tissues were collected, weighed, and counted to determine the percent of the injected dose per gram (% ID/g) of tissue. Data are presented as mean ± standard deviation. *p<0.05; ***p<0.001

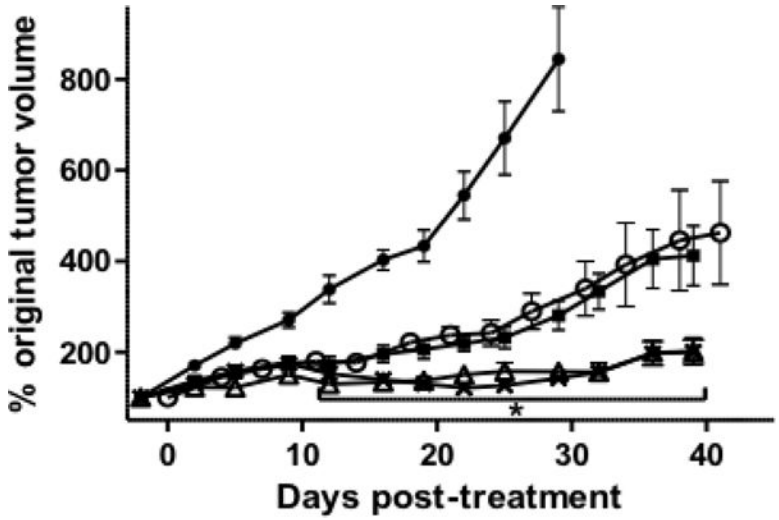

Figure 3.

Tumor growth curves showing the effects of ^{212}Pb-376.96 or ^{212}Pb-F3-C25 on PDX Panc039 tumor growth inhibition *in vivo*. Groups of mice bearing established *s.c.* Panc039 tumors (140–200 mm^3) either were left untreated (filled circles) or injected *i.v.* with 0.46 MBq ^{212}Pb-F3-C25 (open circles) or with 0.36 MBq (filled squares), 0.54 MBq (open triangles), or 0.73 MBq (× marks) ^{212}Pb-376.96 (n = 10/group). Data were plotted as mean percent change (± standard error of the mean) in normalized tumor volume over time relative to the initial volume at the time of injection with the RIC. *$p<0.05$ vs. ^{212}Pb-F3-C25 for the time points indicated.

Table 1

In vitro binding analysis of ^{212}Pb-376.96 to PDAC3 cells.

	K_d ± S.E.M. (nmol/L)	Binding sites/cell ± S.E.M. ($\times 10^4$)	Percent internalized
Adherent PDAC3	9.0 ± 1.1	3.3 ± 0.6	44
CIC PDAC3	21.7 ± 0.7	18.9 ± 2.6	40

Table 2

In vitro inhibition of PDAC3 adherent cells or CIC clonogenic survival by ^{212}Pb-376.96 or ^{212}Pb-F3-C25.

Cells	[a]IC_{50} ± S.E.M. (kBq/mL)	
	^{212}Pb-376.96	^{212}Pb-F3-C25
Adherent PDAC3	41 ± 14	120 ± 12
CIC PDAC3	26 ± 17	180 ± 150

[a]Data are presented as the mean ± S.E.M. of 2–4 individual experiments, with each experiment performed with 4–6 replicate wells.